

Regular Paper

Neural-Net Based Modeling of Velocity and Concentration Fields

Kimura, I. ^{*1}, Yoke, A. ^{*1}, Kaga, A. ^{*2} and Kuroe, Y. ^{*3}

- *1 Osaka Electro-Communication University, 18-8 Hatsu-cho, Neyagawa, Osaka 572-8530, Japan.
E-mail: kimura@isc.osakac.ac.jp
*2 Osaka University, Yamadaoka, Suita, Osaka 565-0871, Japan.
*3 Kyoto Institute of Technology, Matsugasaki, Sakyo-ku, Kyoto 606-8585, Japan.

Received 23 January 2007
Revised 6 June 2008

Abstract : This paper proposes a novel algorithm using an artificial neural network for modeling simultaneously both a 3-D flow velocity vector and a concentration field. The neural network is trained so that four outputted values of the network, three components of a 3-D velocity vector and a concentration of substances such as air pollutants or bacilli, agree with measured ones and additionally the continuity and diffusion equations are satisfied in the flow field. An approximate model for the velocity and concentration field can be constructed in the neural network from sparsely measured data. When any 3-D position, (x, y, z) , is inputted to the neural network model, it outputs a 3-D velocity vector and a concentration at the position. The entire 3-D velocity vector and concentration field, therefore, can be easily estimated using the model. To validate the algorithm, the smoke concentration distribution estimated from a very limited set of measured data is compared with the measured one in which most of the data is unused for the modeling. Even from sparsely measured velocity vectors and smoke concentrations, the novel algorithm gives the entire concentration distribution whose flow characteristics are almost similar to the experimental result.

Keywords : Modeling of Flow Fields, Neural Network, 3-D Velocity Vector, Concentration

1. Introduction

Although 3-D velocity, concentration and temperature fields can be measured in a laboratory (Reungoat et al., 2007; Fujisawa et al., 2008), the whole flow field measurement is very difficult in a real space such as a hospital room, which is always occupied by patients, or a domed baseball stadium, which has a large volume. Airflow distributions are usually measured with some sensors whose measured points are limited in the 3-D space. It is required, therefore, to estimate the entire velocity vector field from sparsely measured data. If some contaminant is contained in the space, the entire concentration distribution should also be estimated. One promising approach for the estimation is to make an appropriate model of the entire field by using some known quantities such as measured data and boundary conditions. Of conventional estimation methods for flow fields, the MASCON (Mass Consistent method) (Dickerson, 1978), which has been very popular in meteorology, and the CFM (Cost Function Method) (Shiota et al., 2000) have been proposed for correcting measured data and interpolating them at the data-lacking points. In those methods, the cost function is minimized by calculus of variations so that the governing equations such as the continuity and Navier Stokes ones are satisfied in the field and also the velocity vectors adjusted according to each algorithm fit the observed (measured) ones.

We present another novel algorithm using an artificial neural network for modeling the 3-D flow velocity vector and concentration field. It is well known that neural networks are excellent tools for realizing 'non-linear smooth mapping'. The neural networks do not require many data for the mapping because they make an

appropriate model by using not a dependent variable as a velocity vector itself but an independent one as a synaptic weight. By introducing some knowledge on characteristic properties such as the mass conservation of air and pollutants (equations of continuity and diffusion), the neural networks can realize effectively an accurate approximation of the velocity and concentration field. In this paper, the neural-net based algorithm is actually applied to an airflow field in the full size model of an infection-free hospital room to evaluate its air purification performance. A smoke diffusion experiment is carried out by using smoke-emitting incense sticks. Velocity vectors and smoke concentrations are measured with a three-dimensional ultrasonic anemometer and a particle counter, respectively. An approximate model for the velocity and concentration field is formed in the neural network from sparsely measured data on velocity and smoke concentration, which are very small in number, and its boundary conditions. The model additionally satisfies the continuity and diffusion equations. The entire 3-D velocity vector and smoke concentration distributions are automatically outputted by inputting all the positions (x, y, z) in the space to the constructed neural-net model. The estimated smoke concentration distribution in the room is compared with the measured one in order to validate the modeling.

2. Neural-Net Based Modeling

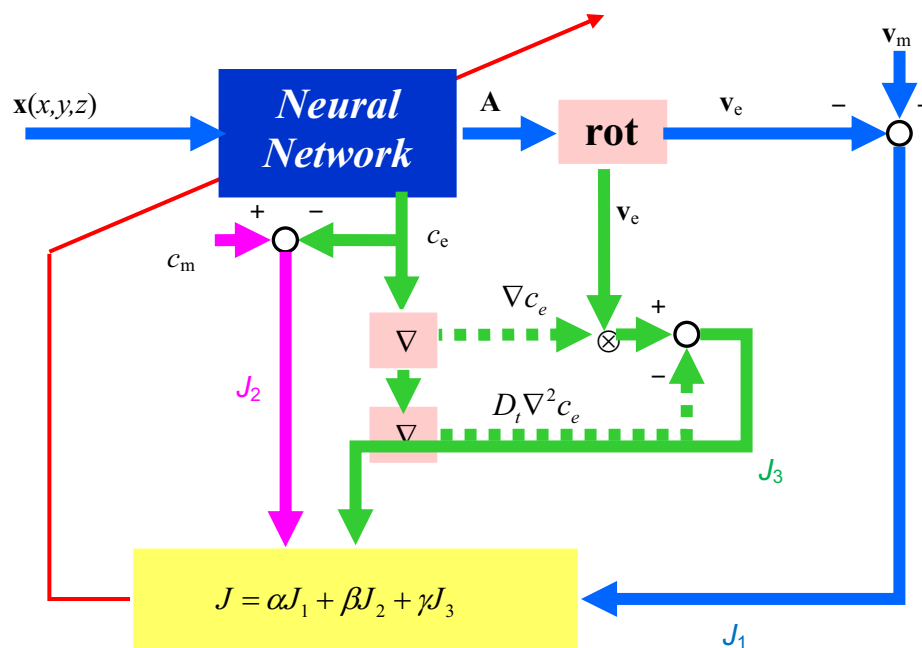


Fig. 1 Neural-net algorithm by 'model inclusive learning'

We propose a novel algorithm using an artificial neural network for modeling the 3-D flow velocity vector and concentration field as shown in Fig. 1. The neural network receives a position vector, $\mathbf{x}(x, y, z)$, and outputs a vector potential, \mathbf{A} , and a concentration, c_e . The relationship between the vector potential, \mathbf{A} , and the estimated vector, \mathbf{v}_e , is defined by

$$\mathbf{v}_e = \text{rot } \mathbf{A} \quad (1)$$

The continuity equation of flow, therefore, is automatically satisfied as follows.

$$\text{div } \mathbf{v}_e = \text{div}(\text{rot } \mathbf{A}) = 0 \quad (2)$$

The performance index on velocity, J_1 , is given by

$$J_1 = \frac{1}{2} \sum (\mathbf{v}_m - \mathbf{v}_e)^2 = \frac{1}{2} \sum (\mathbf{v}_m - \text{rot } \mathbf{A})^2 \quad (3)$$

where \mathbf{v}_m is a measured or a known velocity vector.

The second performance index on concentration, J_2 , is given by

$$J_2 = \frac{1}{2} \sum (c_m - c_e)^2 \quad (4)$$

where c_m is a measured concentration.

The equation of diffusion can be written as

$$\mathbf{v}_e \cdot \nabla c_e = D_t \nabla^2 c_e \quad (5)$$

where D_t is the turbulent diffusion coefficient. The coefficient is simply given as $D_t = 1.0 \times 10^{-2} (\text{m}^2/\text{s})$ whose value is nearly 1000 times the coefficient of kinematic viscosity of air because the coefficient is considered to be high enough for this application. To meet the above equation, the performance index, J_3 , is added as

$$J_3 = \frac{1}{2} \sum (\mathbf{v}_e \cdot \nabla c_e - D_t \nabla^2 c_e)^2 \quad (6)$$

Finally the overall performance index, J , can be obtained by

$$J = \alpha J_1 + \beta J_2 + \gamma J_3 \quad (7)$$

where α , β and γ are weight coefficients, which are determined empirically. The neural network is trained so that the rotation of the vector potential, $\text{rot } \mathbf{A}$, agrees with the measured or the known velocity vector, \mathbf{v}_m , by J_1 , the concentration value, c_e , which is one output of the neural network, agrees with the measured one, c_m , by J_2 , and the diffusion equation is satisfied by J_3 . Accordingly, a 3-D airflow field on both velocity and concentration will be able to be modeled by the neural network in which the flow characteristics of continuity and turbulent diffusion are included. This algorithm is called 'Model Inclusive Learning' (Kuroe and Kawakami, 2007).

The neural network itself is three-layered and is consist of three input nodes, twenty neurons in the hidden layer, and four neurons as the output nodes. To solve the learning problem as mentioned above, we require calculating ' $\text{rot } \mathbf{A}$ ' in the equation (3), ' ∇c_e ' and ' $\nabla^2 c_e$ ' in the equation (6), and the partial derivative of J with respect to the synaptic weight w_{ij} of the network for steepest descent method, $\partial J / \partial w_{ij}$. An efficient algorithm for computing those partial derivatives can be derived by using 'Adjoint Neural Network' (Kuroe et al., 1998).

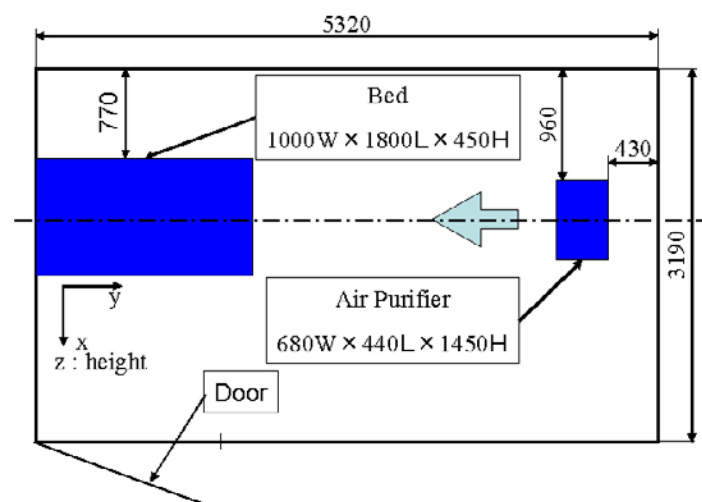


Fig.2 Full size model of an infection-free hospital room

3. Application to an Air-Purified Hospital Room

3.1 Experiment in the Full-Size Model

Figure 2 shows a floor plan of the full-size model of an infection-free hospital room (3190 mm wide, 5320 mm long, 2320 mm high). An air purifier and a bed are set near the right and on the left side wall respectively as shown in the figure. The air purifier has an outlet (620 mm wide, 150 mm high) at the upper part and an inlet (510 mm wide, 300 mm high) at the lower part with a HEPA (High Efficiency Particulate Air) filter. The room is continuously ventilated at the rate of six times the room capacity an hour and continuously exhausted at the rate of twice the room capacity an hour to keep the room pressure lower than the outside one.

3.2 Measurement of 3-D Velocity Vectors

Three-dimensional velocity vectors are measured by moving an ultrasonic anemometer around the middle of the room. Since the instantaneous velocity vectors are partly fluctuating, the measured velocity vectors are given as an average over the time interval of 30 seconds. Figure 3 shows the 3-D velocity vector distribution measured at sixteen experimental points. Such not many measured velocity vectors and known data for some boundary conditions are used for training the network according to the neural-net based algorithm.

3.3 Measurement of Smoke Concentration

In this experiment, we suppose that the room is an infection-free hospital room for tubercular patients. In order to examine how tubercle bacilli exhaled by tubercular patients diffuse over the room, smoke is used instead of the bacilli. The smoke diffusion experiment is carried out by using incense sticks, which are set at eight spots on the floor and six spots on the bed as shown in Fig. 4. Smoke concentrations are measured at 96 equally distant points by moving a particle counter in the middle of the room.

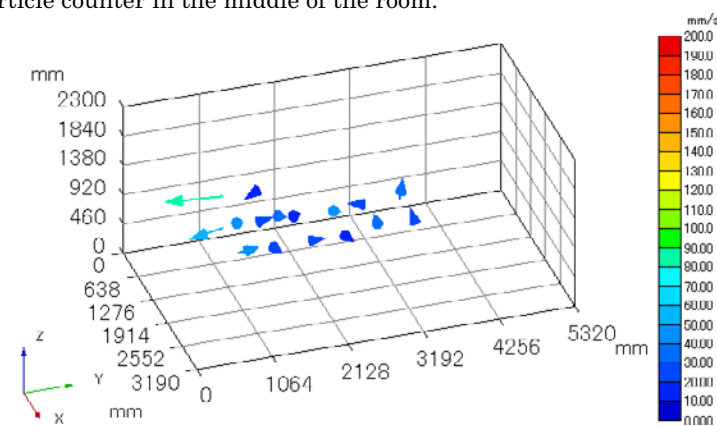


Fig. 3 Measured velocity vectors

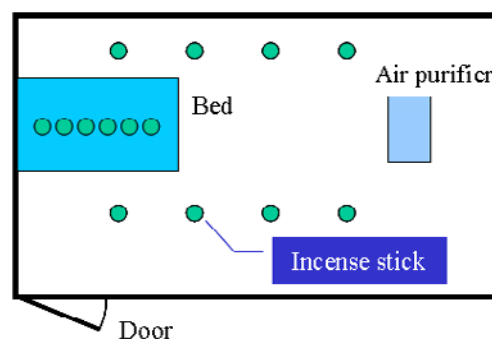


Fig. 4 Smoke diffusion experiment

4. Estimation of Velocity and Concentration

4.1 Desired Outputs of Training Neural Network

The neural network is trained using ‘desired outputs’ so that the overall performance index, J , of the equation (7) reaches a minimum. Sparsely-measured and known values are given as desired outputs. In addition to 16 measured velocity vectors shown in Fig.3, we adopt eight inlet velocity vectors, $\mathbf{v}_m = 0.425$ m/s, and eight outlet velocity vectors, $\mathbf{v}_m = 0.583$ m/s, at the air purifier, and four in-flow velocity vectors into the room through the door gap, $\mathbf{v}_m = 2.41$ m/s. Furthermore, 132 velocity vectors on the walls, $\mathbf{v}_m = 0$ m/s, are added. The sum of desired outputs for velocity vectors is consequently 168. In the case of smoke concentration, we sparsely select 24 measured smoke concentrations, c_m , as desired outputs from all the measured data.

4.2 Estimated 3-D Velocity Vector Distribution

Figure 5 shows the 3-D velocity vector distribution estimated from the neural-net based model and its y-z cross-section. The weight coefficients of the overall performance index, J , of the equation (7) are set at $\alpha=1$, $\beta=\gamma=10$ in this modeling. The previous work on only the 3-D velocity vector estimation (Kimura et al., 2000, 2001) has already proved that the neural-net based algorithm makes the whole field measurement feasible even from a deficient measured velocity field and even if a measured vector field includes many erroneous vectors, a correct velocity vector field is reconstructed from measured data with noise (erroneous vectors). In the figures, a fresh air flow blows out of the outlet of the air purifier and its flow turns obliquely upward. Then the flow goes downward along the left wall near the bed and runs along the bed into the inlet of the air purifier. It means that the flow could bring tubercle bacilli into the air purifier where more than 99.97 % of the bacilli are caught by the HEPA filter.

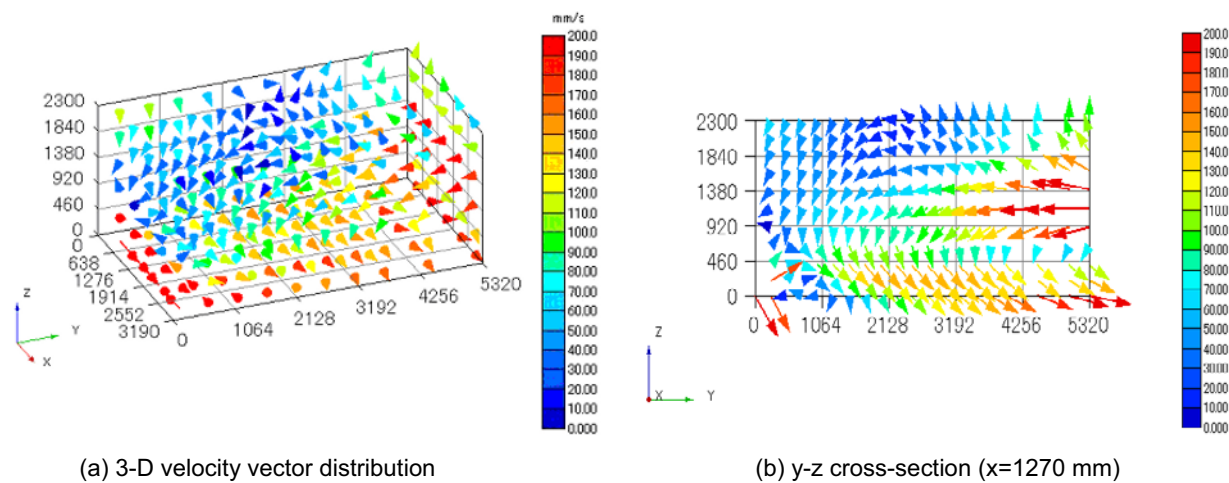


Fig.5 Estimated velocity vector distribution

4.3 Comparison between Measurement and Estimation on Smoke Concentration

The smoke concentration distribution in the room is estimated using the neural net based model, and then compared with the measured one in order to validate the proposed algorithm. Regarding ‘diffusion’ as important in this paper, the weight coefficients of the overall performance index are set at $\alpha=1$, and $\beta=\gamma=10$. Figure 6 shows the x-y cross-sections ($z = 1500, 1000, 500$ mm) of the measured and estimated smoke concentration distributions. The concentration value is normalized by the mean value at the inlet of the air purifier. As the measurement area is limited to 1940 x 3500 mm in the x and y directions, the estimated distribution is constructed using the values estimated at the same positions as 96 measured ones. All the estimated results grasp the experimental diffusing behavior on the whole. The smoke emitting sources on the bed are also clarified in the figure (c).

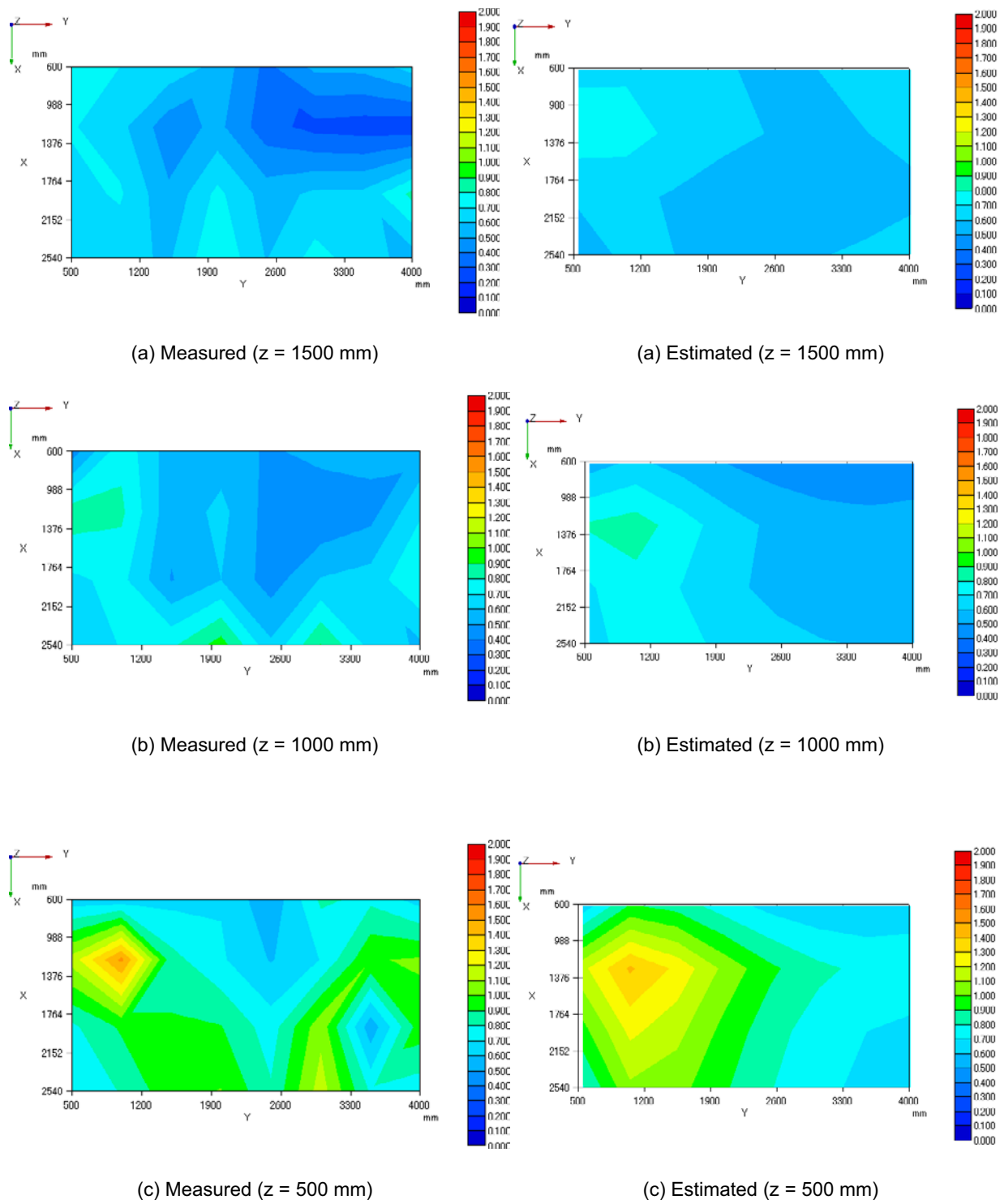


Fig.6 Comparison of estimated and measured smoke concentration distributions

4.4 Estimated Smoke Concentration Distribution in the Entire Field

Figure 7 shows the smoke concentration distribution estimated in the entire field (3190 x 5320 mm). The x-y cross-sections ($z = 1500, 1000, 500$ mm) and the y-z cross section ($x = 1270$ mm) are given in the figure. The x-y and y-z cross-sections are constructed from 3,185 and 2,385 estimated data respectively. The estimated distribution shows that the smoke concentration is high near the bed ($z = 500$ mm) and floor ($x = 1270$ mm) where the incense sticks are set and low in the upper part of the room. Even though any information on the smoke emitting sources is not given when modeling, these sources on the bed and floor appear clearly.

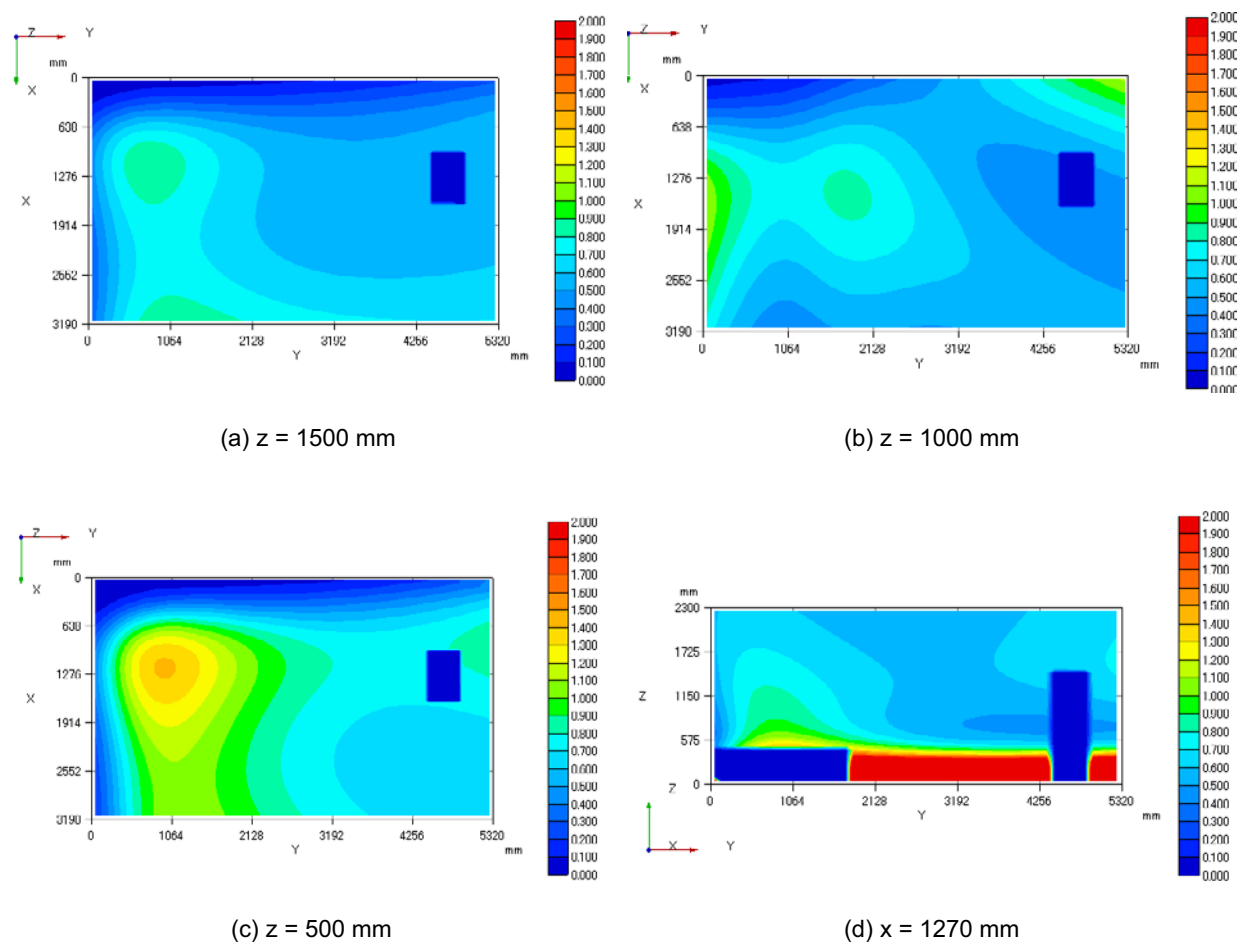


Fig.7 Estimated smoke concentration distribution in the entire field

6. Conclusion

The whole flow field measurement is unavailable in such a real space as a hospital room or a domed baseball stadium. An appropriate flow field model can be constructed from sparsely measured values by the proposed neural-net based algorithm, thereby estimating effectively the entire flow field on 3-D velocity and concentration. The constructed flow field additionally satisfies the equations of continuity and diffusion. The proposed neural-net based modeling will be consequently an effective way to evaluate the effectiveness of air purification in the air-purified spaces where the whole field measurement is extremely difficult. Even if the emitting sources of substances such as air pollutants and bacilli are unknown, they will be clarified from its estimated distribution.

References

- Dickerson M H. MASCON-A Mass Consistent Atmospheric Flux Model for Regions with Complex Terrain. *Journal of Applied Meteorology*, 17-3 (1978), 241-253.
- Fujisawa N, Watanabe M and Hashizume Y. Visualization of Turbulence Structure in Unsteady Non-Penetrative Thermal Convection Using Liquid Crystal Thermometry and Stereo Velocimetry. *Journal of Visualization*, 11-2 (2008), 173-180.
- Kimura I, Morino T, Furukawa T, Kaga A and Kuroe Y. Estimation of Three-Dimensional Velocity Vector Fields Using Neural Networks. *CD ROM Proc. of the Millennium 9th International Symposium on Flow Visualization*, 166.1-9, (2000).
- Kimura I, Morino T, Furukawa T, Kaga A and Kuroe Y. Neural Net-Based Reconstruction of 3-D Velocity Vector Fields from Deficient Measured Data. *CD ROM Proc. of the 3rd Pacific Symposium on Flow Visualization and Image Processing (PSFVIP-3)*, F3125, (2001).
- Kuroe Y, Mitsui M, Kawakami H and Mori T. A Learning Method for Vector Field Approximation by Neural Networks, *Proc. of 1998 IEEE International Joint Conference on Neural Networks (IJCNN'98)*, 2300, (1998).
- Kuroe Y and Kawakami H. Vector Field Approximation by Model Inclusive Learning of Neural Networks. *Artificial Neural Networks - ICANN 2007, Lecture Notes in Computer Science*, 4668, Springer-Verlag, (2007), 717-727.
- Reungoat D, Riviere N and Faure J.P. 3C PIV and PLIF Measurement in Turbulent Mixing -Round Jet Impingement-. *Journal of Visualization*, 10-1 (2007), 99-110.
- Shiota T, Yamaguchi K, Kaga A, Kondo A and Inoue Y. Combined Technique of PIV and CFD Using Cost Function and Comparison with FDDA. *CD ROM Proc. of the Millennium 9th International Symposium on Flow Visualization*, 205.1-9, (2000).

Authors Profile



Ichiro Kimura: He received his M.S. degree in instrumentation engineering from Kobe University, Kobe, Japan in 1972 and his D.E. degree in mechanical engineering for industrial machinery from Osaka University, Osaka, Japan, in 1983. He was a Research Associate from 1972 to 1984 and an Associate Professor from 1984 to 1993 of Instrumentation Engineering at the Faculty of Engineering, Kobe University. He is currently a Professor of Mechatronics at Osaka Electro-Communication University, Osaka, Japan. His current research interests are Neural-net Based Quantitative Flow Visualization and Modeling of Visual Neuron.



Akihiro Yoke: He received his B.S. degree in electromechanical engineering in 2005 and his M.S. degree in mechanical and control engineering in 2007 at Osaka Electro-Communication University, Osaka, Japan.



Akikazu Kaga: He received his B.E. degree in 1969, his M.E. in 1971 in Mechanical Engineering, and his D.E. degree in 1985 in Environmental Engineering from Osaka University. He has been working in Osaka University from 1971 as a research associate, from 1988 as an associate professor and from 2000 as a professor. His current research interests are Airflow Measurement using Flow Visualization and Image Processing, and the Analysis of the Behavior of Detrimental Chemicals in the Environment.



Yasuaki Kuroe: He received his Ph.D. in industrial science from Kobe University, Kobe, Japan in 1982. In the same year he joined the faculty of Department of Electrical Engineering, Kobe University as a Research Associate. In 1991, he moved to Kyoto Institute of Technology as an Associate Professor and he is currently a Professor at the Department of Information Science, Kyoto Institute of Technology, Kyoto, Japan. His research interests are in the areas of Neuro-Computing and Computational Intelligence, Control Theory and its Application, and Computer-Aided Analysis and Design.